



Peer review status:

This is a non-peer-reviewed preprint submitted to EarthArXiv.

1 **Noisy Sampling Inherent to Daily Precipitation Observations**
2 **and Implications About Return Level Inferences**

3 Alexander Weyant,^a Anna Panorska,^b Alexander Gershunov,^a Rachel Clemesha,^a

4 ^a *Scripps Institution of Oceanography*

5 ^b *University of Nevada, Reno*

6 *Corresponding author:* Alexander Weyant, awayant@ucsd.edu

This work has been submitted to Journal of Applied Meteorology and Climatology. Copyright in this Work may be transferred without further notice.

7 ABSTRACT: Daily precipitation observations form the backbone of the United States precipita-
8 tion network. However, precipitation is episodic over minutes and hours and is (seasonally) diurn-
9 ally driven, which immediately raises questions about the statistical characteristics of its extreme
10 daily accumulations in general. Atop this is layered troubling context: during the historical period
11 of these observations (1948-present), the scheduled time of day when precipitation accumulations
12 are recorded has varied by the type of weather station as well as over time, raising the dual spectres
13 of statistical model misspecification and temporal inhomogeneity. We explain the subtle character
14 of this particular confounder of observations, conduct a paired experiment intended to quantify
15 the magnitude of the inhomogeneity it may induce, and further explore some first consequences of
16 the attendant misspecification affecting extreme values. While the model misspecification is not
17 shown to affect inferred trends in extreme precipitation, we find that the estimated uncertainty of
18 large return levels of the daily precipitation distribution is typically underestimated, and further-
19 more that the tail of the distribution has less to do with precipitation itself than previously thought.
20 Ultimately, this means that tails of daily precipitation distributions are easily over-interpreted, that
21 existing spatial interpolations of the tails have an ambiguous physical meaning, and moreover that
22 daily accumulations, despite being the most common historically, provide only a muddled view of
23 the underlying physical-stochastic process driving precipitation itself.

24 1. Introduction

25 Whether we are designing infrastructure, interpreting the present, or making projections about
26 the future, it is crucial to understand the magnitude of exceptional floods. For any physical hy-
27 drological model (and for most conceivable statistical models) precipitation figures into both the
28 antecedent conditions and acute drivers of floods. Therefore, properly characterizing the magni-
29 tude and character of heavy precipitation events is of great practical importance.

30 None of the above has been well-defined, and this is to demonstrate that the issue at hand, at its
31 heart, is one of defining an interpretive framework well suited to limited data we have in order to
32 solve a practical problem. The technical implementation is subordinate to the framework. Case
33 in point, statistical inference on daily precipitation data is only attempted because of an underly-
34 ing belief that it is technically possible and that it provides something beyond what intuition or a
35 naive, direct reading of the input data would would. It is technically enabled by probability theory,
36 mathematical statistics, a long-term weather observing network, and computing power. But no-
37 body would be arguing about its technical implementation (e.g. distributional forms or optimality
38 properties of estimators applied to small samples) without the underlying belief that it is a useful
39 approach in the first place. Whether or not this belief is rational, the powers that be demand sim-
40 plistic, replicable, *quantitative* answers to hopelessly complicated questions [St. Laurent (2020);
41 CalTrans (2020); CA DWR (2012)]. This animates a reductive interpretive framework, which pro-
42 vides *an* answer alongside a measure of its uncertainty. The estimate of this uncertainty, as it tends
43 to be interpreted in practice, is illusory.

49 This article deals with the issue apparent in figure 1. Most longterm precipitation records con-
50 sist of once-daily measurements, taken on a fixed schedule. Apparently, the time of day when a
51 raingauge is checked (**T-Obs**) can strongly affect our estimates of the probabilities of large precipi-
52 tation totals and their attendant uncertainties. Fifty-five years of hourly data available at Farmland,
53 Indiana¹ exemplifies this point. The observed overall maximum daily accumulations at midnight
54 and 17:00 local time are about 110mm and 140mm, respectively. A roughly 30mm difference
55 over the average of these two comes out to a relative difference of about $1/4$. When a general-
56 ized extreme value (GEV) distribution is fit to annual maxima of each daily series at the same
57 site, the theoretical estimates of return levels differ by about the same amount. In this sense, the

¹A Global Historical Climatological Network (GHCN) site with exceptionally digitized metadata, beyond what is seen at most official “first order” National Weather Service (NWS) or Weather Bureau Army Navy (WBAN) sites. See **Appendix A: Data**

Two Daily Precip Return Level Curves

Farmland, Indiana; ID: USC00122825

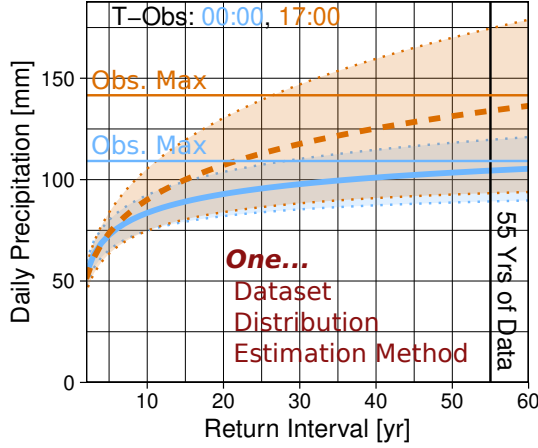


FIG. 1. Estimated return level (RL) curves of daily precipitation for the GHCN-daily station Farmland 5 NNW, In (ID: USC00122825) outside the town of Farmland in eastern Indiana; The solid (blue) curve is from daily observations taken at midnight local time and the orange (dashed) curve is likewise for 5pm. Corresponding $\alpha = 1/20$ confidence intervals for RLs are calculated with the delta method Bickel and Doksum (2015), see **Extreme Value Inference**.

GEV distribution and parameter estimation are doing their job within their own context. However, the qualitative behaviour of confidence intervals, is pathological for those who overgeneralize the meaning of confidence intervals to be akin to a general measure of uncertainty.² The inference from the midnight-recorded series would lead somebody to believe that the 50y return level is well understood after 55 years, while the 17:00 inference leaves a completely different impression. This is illustrative of a broader problem arising from daily observations being taken at various times of day on a spatially dense, longterm, volunteer-operated precipitation observing network in the United States.

We begin by providing a high level overview of a common framework for estimating the probability of rare precipitation accumulations. Nothing here is new, but taking these standard procedures for granted and removing them from their context is precisely how the problem at hand arose. After considering particular ways the procedure may be thwarted by the randomness in-

²Although this is a pervasive notion, it is both unkind and unproductive to call out individual people through citations. In addition, people making these kinds of errors are in fact the least likely to lay out their assumptions explicitly in writing. A couple of examples from engineering manuals are discussed in the discussion.

duced by our daily sampling rate, we present the results of experiments and explorations probing these vulnerabilities. We conclude by offering some interpretations and suggestions for a way forward.

a. Models and their Misspecification

Reductionism sometimes gets a bad rap, but it is precisely what makes the problem seem tractable, and therefore prevents resignation or paralysis. An added benefit is that the reduction leads to a formal procedure, making the results “objective” in the sense that the output is a function of the input, regardless of the opinions or disposition of the person conducting the procedure. This enables standardization which is required by regulations. Engineering depends on it.

Extreme Value Theory (**EVT**) is at the core one such reductive framework, which allows us to convert the herculean problem of extrapolation to one of mere numerical optimization. The underlying mechanics are those of typical statistical inference: the limited input data are considered alongside a chosen family of probability models, which become proper distribution functions once the parameters’ values are specified. To be quite explicit, the role of EVT itself is in selection of the Generalized Extreme Value (**GEV**) distribution as the family. Without a theory to select a family, there would be no formal basis for shoehorning the problem of extrapolating precipitation to the scale of the historical record and beyond into a numerical optimization routine. Once the family is selected, standard estimation techniques can proceed, and the machinery of estimation theory furthermore furnishes a sampling distribution which provides confidence intervals.

But these point estimates and intervals only convey meaning in context. A model misspecification occurs when the assumptions underpinning the inference procedure are violated. We focus on the GEV because of its widespread adoption. It is used in NOAA’s Precipitation Frequency Atlas [Perica et al. (2011)], which is a basic, trusted source of extreme precipitation estimates for many practical applications [St. Laurent (2020); CalTrans (2020)]. For those familiar with the issues of GEV, we ask that you suspend your disbelief. The misspecification we present extends beyond it.

Recapitulating³, the observed block (annual/seasonal) maxima of daily precipitation $\{y_t\}$, where t indexes the blocks⁴, are assumed to be realizations Y . This is written as $y \sim Y$. The random variable Y is characterized by Cumulative Distribution Function (**CDF**) F . It is a function of y .

³But only in the minimal generality to make the point.

⁴ t could be “June, July, August 2025”

$F(y)$ is the probability that the annual maximum of daily precipitation is less than y . Now, F is conceptualized as member of a set of functions $\mathcal{F} = \{F_\theta \mid \theta \in \Theta\}$, where θ are parameters and Θ is the set of values they could potentially take. Notably, \mathcal{F} is comprised of functions of a particular form⁵. The great reduction hinges on the choice of the family. Once a family is chosen (e.g. normal/Gaussian), the value of θ alone defines the CDF, so the practical goal changes to inference of the puppetmaster behind the curtain θ (e.g. mean and variance).

The choice of family depends on background knowledge about the process which generated the data. This is where EVT, Large Deviation Theory, or physical reasoning enter the picture [e.g. Coles (2001); Veneziano et al. (2009); Wilson and Toumi (2005), respectively]. Regardless of the choice of \mathcal{F} , the ultimate result is that $y \sim Y$ and $F_\theta(y) = \mathbb{P}(Y \leq y)$. No matter how technically advanced a distribution is and regardless of whether the underlying physical reasoning is sound, a fundamental oversight in how the data was recorded can foil our understanding the the physical process which is truly the object of our studies.

b. The Factor Unaccounted For

At Farmland, Indiana, around the time the largest ever 24hr total was recorded, precipitation occurred in three bouts separated by a few hours of (locally) dry weather (Fig 2a). The first wet bout occurred around noon on 21 August, the second just before midnight, and the third in the morning on 22 August.⁶ That causes a strong dependence of the recorded 24hr totals on the daily T-Obs (Fig 2b). The 24hr total recorded at 17:00 includes only the first wet event and the one recorded at midnight includes only the first two wet events in the total for August 22. Neither of them provides the total of the entire precipitation event. Finally, note in long-term, spatially dense records, we typically only have access to daily observations, so that the whole range of possible valid measurements would be unknown in general (Fig 3b vs. c). This constitutes a hidden, irreversible, nonlinear transformation of the data from the moment it is collected.

This is so for any particular daily value, so this propagates to the annual maxima of daily precipitation, which further results in mischaracterization of the extreme/large 24hr precipitation values

⁵For example, the CDF of a normal distribution is a member of the family $\left\{F(y) = \frac{1}{2} \left[1 + \operatorname{erf} \left(\frac{y-\mu}{\sigma\sqrt{2}} \right) \right] \mid (\mu, \sigma^2) \in \mathbb{R} \times \mathbb{R}_+ \right\}$. Please excuse the poor set notation.

⁶The National Weather Service (NWS) provides further metrological and climatological context. See <https://perma.cc/T9HA-8TSD> and <https://perma.cc/JN48-CBY4>.

Context of the Largest 24hr Precip Total
FARMLAND, IN; ID: USC00122825

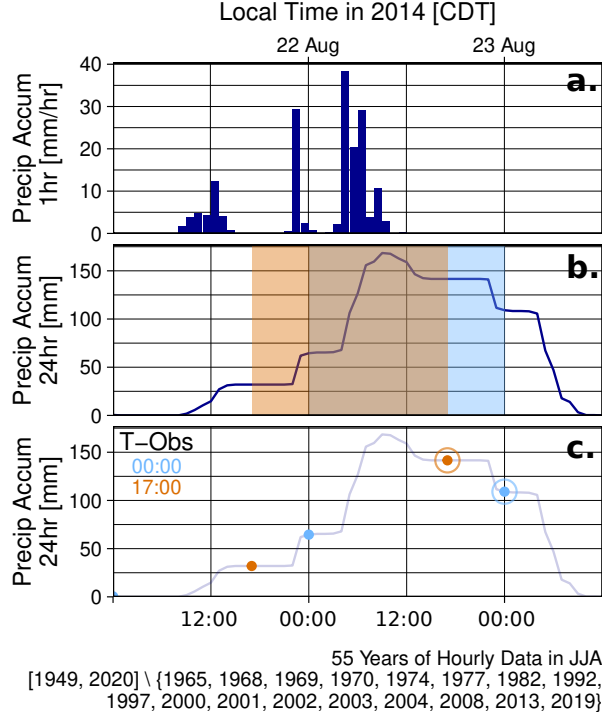


FIG. 2. An overview of the daily-record-setting precipitation event since 1949 at Farmland Indiana; a) the hourly accumulations, b) the corresponding 24hr accumulations, with time intervals contributing to the largest 5pm and midnight totals highlighted in orange and blue, c) two sets of points (5pm - orange, midnight - blue) which typical daily observations at this site would reveal

derived/estimated using statistical methods like the AMS-GEV.⁷ Ultimately, the recorded annual maximum daily total is a random proportion of the actual annual maximum 24hr total, which could be as small as $1/2$ of the actual 24hr maximum. We call this random proportion the **discretization factor**.

Definition 1.1 (Discretization Factor). *If $P_{h,d}$ are the 24hr precipitation accumulations for $T_{Obs} = h$ and days d in a block, then $r_h = \frac{\max_d \{P_{h,d}\}}{\max_{h,d} \{P_{h,d}\}}$ is the discretization factor for the block maximum of observations taken at $T_{Obs} = h$.*

⁷At this station, the issue is also quite prominent if we consider the all-time record value of daily precipitation. The 24hr running total varies within this event, but it is furthermore so that this particular 24hr curve is record-setting for all hours of the day, except 23:00.

Note, that r_h is a random quantity or more formally a realization of a random variable (**RV**). When we consider it as a random variable, we denote it R_h or simply R . Further, we can write any recorded daily annual maximum y as the product of the actual annual maximum 24hr precipitation total x and the discretization factor as $y = r_h x$, which makes explicit the fact that the recorded daily totals do not really provide accurate information about 24hr accumulations. In turn, that implies that whatever statistical methodology we use for the analysis and modeling of maximum daily precipitation records, the results will not accurately reflect the maxima of the actual 24hr accumulations. Most importantly, the errors of any prediction or estimation which do not take r_h into consideration will not be accurate measures of uncertainty.

c. The Discretization Factor & the Diurnal Cycle

If it turns out that R_h is dependent on the T-Obs itself, then it potentially brings about a trend-inducing inhomogeneity [Domonkos (2024) for an overview] in the US precipitation network, as the suggested T-Obs has changed from evening to morning over the decades [supplementary table S1, supplementary figures S1, S2]. A quite simplistic look at hourly precipitation observations reveals a diurnal cycle in Summer (JJA) which weakens into the shoulder seasons (MAM, SON) [Fig. 3]. We demonstrate the effect of R on GEV family-based estimates (**Extreme Value Inference**) of annual exceedance probabilities for daily precipitation as well as this potential inhomogeneity. Notably, a model-data driven GEV approach requires the estimation of a shape parameter ξ , which pertains to, among other things, the propensity of the annual maximum process to produce large outliers. There is no mere multiplicative scale factor (simple bias correction) which can account for a change in shape.

2. Experiments, Explorations, and Their Results

We perform a series of demonstrations: “experiments” whenever possible and “explorations” otherwise. The experiments have clearer hypotheses and control conditions, while the explorations we included are the most practical and cogent results of our broader exploratory analysis. Exploration 1 and experiment 1 were performed with the suspicion that an inhomogeneity may be affecting the record. Exploration 2 was conducted afterward in an effort to interpret what had come before. Experiments 2 and 3 were performed in light of some assumptions made in literature

Detected Diurnal Cycles in Measureable Hourly Precipitation

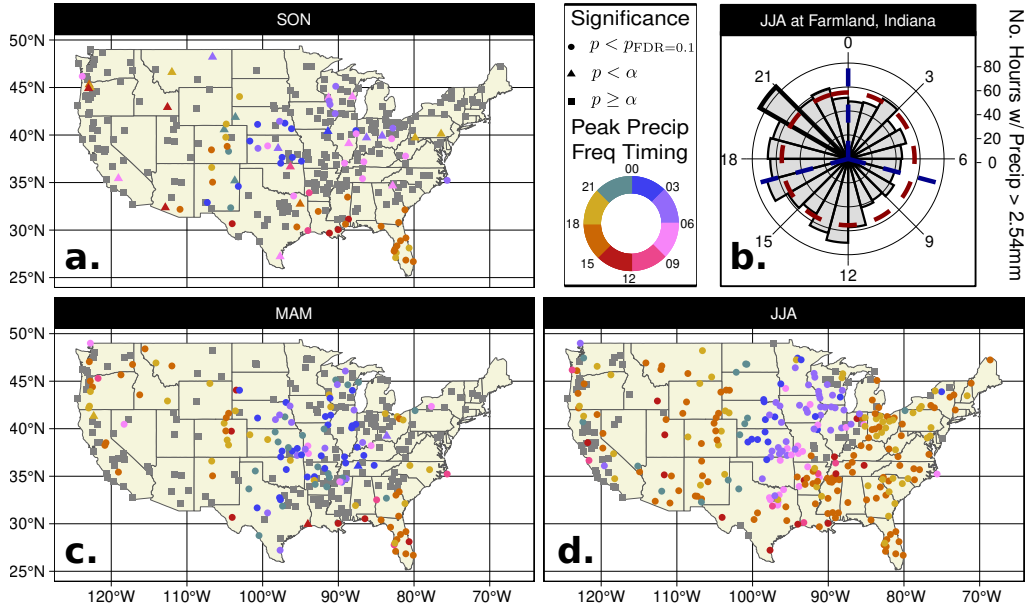


FIG. 3. Scatterpoint map of CONUS showing the observed diurnal cycle in hourly precipitation in seasons SON (a), MAM (c), and JJA (d). DJF was omitted due to a lack of diurnal cycles. Binned colors, which divide the day into 3 hour sections, correspond to the most frequent hour of measurable precipitation. Significant ($FDR = 0.1$), "marginally significant" ($\alpha = 0.05$), and non-significant ($\alpha \geq 0.05$) diurnal cycles are denoted with circles, triangles, and squares, respectively [Benjamini and Hochberg (1995); Wilks (2016)]. $p_{FDR=0.1}^*$ was calculated separately for each season. The test was one-sided and the statistic was the mean squared difference of the hourly frequency from the average across the 24 hours. The 250 replicates for the null hypothesis of "no diurnal cycle" were created by assigning random start times to every observed historical instance of 24hr precipitation exceeding a low threshold of 2.54mm, the observing resolution of the coarsest transcribed data. Points without significant diurnal cycles are coloured grey. (b) shows the observed diurnal frequencies for Farmland, Indiana. The mean over all 24 hours is shown as a dark red dashed circle.

[Papalexiou et al. (2016) and references therein] we had found after doing the bulk of our work. The literature contains strong assumptions which we had already taken to be unreasonable.

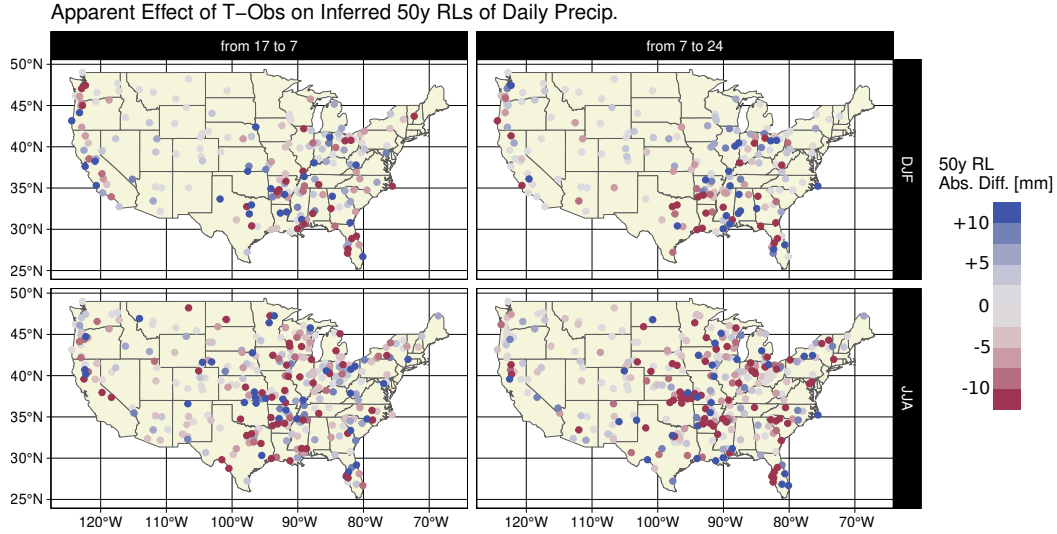


FIG. 4. Absolute differences [in mm] between 50 year return levels of daily precipitation accumulations, inferred under different T-Obs in winter and summer; The estimates are the result of a maximum likelihood estimation of stationary parameters of a GEV distribution. See **Extreme Value Inference**.

a. Exploration 1: T-Obs and Stationary Inference of Responses

Setup: If the T-Obs changes, what is the magnitude and direction of the effect on our inferences? The extreme value inferences which matter most to the “end user” are the return levels of rare events (large quantiles) as well as their uncertainty. A straightforward way of looking at this is to aggregate hourly precipitation into 24 hour totals, then estimate large (50 year) return levels of daily precipitation assuming different T-Obs (07:00, 17:00, and 24:00 local time)⁸. We explore both the differences between these inferences of quantiles and compare them to a baseline of sampling variability, with the sensible yet vague null expectation⁹ that the baseline variability ought to dominate the inferred treatment-induced differences we observe.

Result: Figure 4 shows differences on the native scale of the responses, inferred at common observation times. Figure 7a shows this for 24 potential T-Obs at Farmland, Indiana. Absolute values over 10mm (about $\frac{1}{2}$ inch) are common. In absolute and relative terms, this is consequential, especially given that these differences arise purely from slightly different views of identical input data. Airports mostly have a midnight T-Obs while most other manual raingauges to which

⁸07:00 (morning) and 17:00 (evening/sunset) are based on historical recommendations for volunteer observers. 24:00 (midnight) is most common for Airports and is common for sites with recording gauges. See supplemental section **T-Obs in the CONUS Raingauge Network**.

⁹Recall, this is an exploration, not an experiment.

T-Obs Change	Season	% s.t. $ \hat{r}_{50,b} - \hat{r}_{50,a} /\hat{\sigma}_{r_{50,a}} > 1$
From 17 to 7	SON	19
	DJF	29
	MAM	21
	JJA	13
From 7 to 24	SON	21
	DJF	22
	MAM	22
	JJA	16

TABLE 1. Portions of raingauges for which the absolute standardized differences of inferred 50yr return levels exceeds 1. Heuristically, these values may be compared to 32%, approximately the value that would arise if a large number of inferences from independent samples under the original distribution were compared to the original value.

they would be compared have morning or evening T-Obs [Supplemental Figure S1]. One notable consequence of this is that differences in inferences between Airport and Cooperative Observer (COOP)¹⁰ sites could easily be interpreted as consequences of more quantifiable and physically sensible site characteristics: orography, the availability of moisture from evapotranspiration, or perhaps effects of aerosols. The paired exploration shows that if T-Obs alone is manipulated, there are rather spatially coherent differences induced in our inferences. However, we must keep in mind that the spatially coherent splotches in figure 4 themselves would not manifest in daily data. Rather, the station type and, to a lesser extent, the year determines the T-Obs for us.

How do these differences compare to purported standard errors? Table 1 shows that, at a minimum (in JJA, with a change from 5pm to 7am), about 13% of raingauges have differences in 50yr return level inferences which are larger than the standard errors. On the higher end, this is 29% of gauges for DJF, which should be taken with a grain of roadsalt, given the difficulties of measuring precipitation under freezing and windy conditions. Overall, we can say that about 20% of gauges have differences which are comparable with standard errors. Heuristically, about 32% would be expected to have differences of this magnitude or larger, given completely independent, novel samples arising from the distributions inferred on the base (“from”) T-Obs. Overall—and mind you, vaguely— this means the randomness induced by the daily sampling process itself

¹⁰Volunteer-operated raingauges.

(R), at these particular hours, is almost as large as that which would otherwise be attributed to precipitation itself (X).

Two immediate upshots: (i) precipitation itself may not be as volatile as we believe it to be and that (ii) if the differences we see are structurally related to the diurnal cycle, then changing T-Obs in the middle of the record may induce spurious trends.

b. Experiment 1: T-Obs and Trends

Setup: Experiment 1 is based on the following intuition: if there are two distinct methods of observing the same value, each with their own precision level, and if the difference between these observations is at all comparable in magnitude to said precision, then switching from one observing method to another over time may introduce spurious trends which interfere with our ability to detect actual trends in the quantity we want to track.

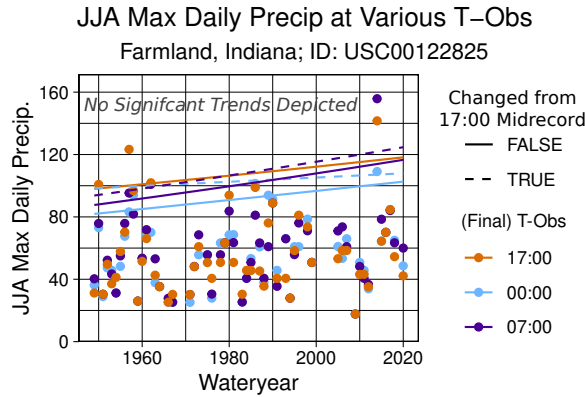


FIG. 5. JJA maxima series for daily precipitation with T-Obs 17:00 (orange), 00:00 (blue), and 07:00 (purple); Overlaid are lines of various nonstationary GEV 20y RL estimates. The location and scale parameters vary linearly with the year. Solid lines correspond to daily observations held at a given T-Obs throughout the entire record, and dashed lines represent the condition of switching from 17:00 to other times midway through.

Observing daily precipitation at various times of day provides various views of the same dataset. Wherever the results of Exploration 1 show sizeable differences between inferences on these views, we may expect to find trends which are not present in the more common daily data. The opposite may also be true, depending on the agreement in signs of the induced and actual physical trends.

234 In this experiment, we estimate coefficients of a simplistic vector generalized linear model
235 (**VGLM**) on the block maximum series of daily precipitation under a few conditions, which corre-
236 spond to different histories of T-Obs throughout the record. The first condition is that the daily data
237 are as provided by the observers, which contains a mixture of T-Obs, the composition of which
238 is not always known. The next three conditions correspond to hourly precipitation aggregated
239 daily resolution at 07:00 (morning), 17:00 (evening) and 24:00 (midnight). The last two are meant
240 to represent the nearly “worst case”¹¹ scenario for the potential inhomogeneity: a change in T-
241 Obs (evening \rightarrow morning and evening \rightarrow midnight) is imposed simultaneously and unanimously
242 across the network, precisely in the middle of the record.

243 We specify that the VGLM’s likelihood is of the GEV family, with the shape being held con-
244 stant, but with the location and scale linearly related to the year. A trend in the block maximum
245 series (**BMS**) in either direction is detected whenever the null hypothesis that the location slope
246 coefficient is 0 is rejected in a likelihood ratio test.

247 There are many potentially interesting comparisons to make on the outcomes of this. We con-
248 sider the number of stations which had trends under each condition, as well as the counts of
249 disagreements about the same precipitation records under the various treatments. We consider
250 whether or not (i) 24hr precipitation records (aggregated hourly records), being free of this par-
251 ticular inhomogeneity by construction, would have trends more or less often than the raw daily
252 data, (ii) whether inferred trends are specific to the T-Obs, and (iii) whether switching the T-Obs
253 mid-record would induce spurious trends which interfere with any actual trends.

270 **Result:** Table 2 indicates that there is not much to see here, when we consider inferred trends
271 on the location and scale of the GEV distribution. It may seem counterintuitive, given the out-
272 come of Exploration 1 and the intuition behind this experiment. BMS trends at Farmland, Indiana
273 (Fig. 5) show that, while the intuition behind the experiment is well-founded, the T-Obs-induced
274 inhomogeneity is typically not strong enough to affect decisions about the significance of trends.
275 Note that the slope of the 20y RL under the 17:00 \rightarrow 00:00 condition (blue dashed line) is rather
276 flat compared to either the pure 17:00 or 00:00 lines (solid orange and blue lines). The pure 17:00
277 line sits about 20mm above the 00:00 line throughout the record. They are nearly parallel, and

¹¹In the sense of ubiquity across the network. Based on the actual history of T-Obs in the network [Supplemental Table S1], we already know that the network did not simultaneously, unanimously, and permanently switch T-Obs.

¹⁴There are no false discovery rate considerations in this case, especially given the small number of stations and the fact that we are not claiming an affirmative result.

Season	No. St.	Dly.	17	Dly., not 17	17:00, not Dly.	17 to 07	17 to 24
SON	88	13	9	5	1	10	11
DJF	88	5	6	3	4	5	11
MAM	88	11	10	6	5	10	11
JJA	82	12	8	7	3	4	5

TABLE 2. Representative results of the paired T-Obs change experiment for linear GEV location and scale parameters’ trends. For each season, the total number of stations is reported, followed by the number of stations for which a (marginally) significant ($\alpha = 0.05$)¹⁴slope of scale and locations parameters were inferred on the daily data and the hourly data aggregated daily (“Dly.”) at 17:00 (“17”). The next two columns (“A not B”) report disjunctions of these counts, the number of stations with trend detected in natively daily data and no trend in 24hr accumulations subsampled at 17:00, and vice versa. The last two columns (“A to B”) report the number of stations with significant location trends under the conditions that the T-Obs changed halfway through the record.

switching between daily observational datasets midway through the record period results in a line with a slope about $1/2$ of either of those of the pure sets. This being said, *none* of these trends are considered significant in the first place, so they do not contribute to the counts in Table 2. Ultimately, how to interpret this depends on whether we opt to believe our own lying eyes or the result of a null hypothesis significance test. It seems that while this particular decision rule is resistant to the inhomogeneity, any interpretation of the magnitude of a trend should be undertaken very cautiously [Figure 6].

c. Exploration 2: T-Obs and Stationary Parameter Inference

Setup: Uncertainty of parameter estimates is usually quantified in terms of a covariance matrix $\widehat{\Sigma}$ of our estimator $\widehat{\theta}$. However, this only quantifies uncertainty of a particular kind, that of the sampling distribution of the estimator $\widehat{\theta}$, which arises from *independent* replicate samples of the same process. If $\widehat{\theta}_o$, our estimate of the supposed true θ is unbiased (or roughly so), then the magnitude of the differences $\|\widehat{\theta} - \widehat{\theta}_o\|$ are placed in the context of covariance matrix $\widehat{\Sigma}$. In particular, $\widehat{\theta} \sim \text{MVN}(\widehat{\theta}_o, \widehat{\Sigma}_o)$ ¹⁵ under asymptotic (large-sample) properties of maximum likelihood es-

¹⁵Multivariate Normal (MVN)

Putative Magnitudes of Detected Changes in 20y RLs

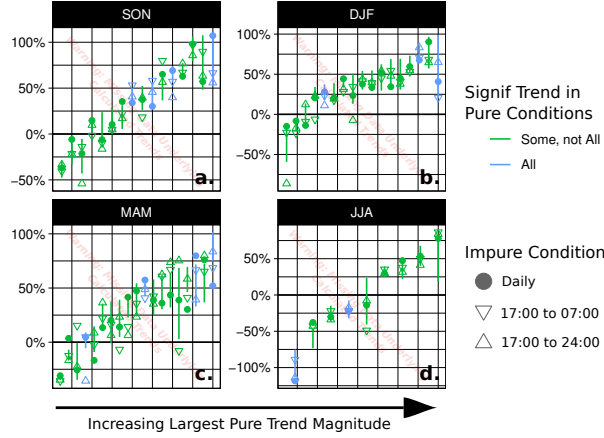


FIG. 6. Magnitudes of detected trends of 20y return levels, expressed as return level in the final year minus return level in the first year divided by the mean over all years; Each vertical line segment corresponds to a raingauge where at least one marginally-significant ($\alpha = 1/20$) trend was detected. The line segments denote the min and max magnitude for each station, the solid dots show the corresponding daily value, the up-pointing triangle the switch condition 17:00 \rightarrow 24:00, and the downward pointing triangle 17:00 \rightarrow 07:00. Due to missing data in many of the series, the magnitudes of these trends are not to be taken outside of their context. See **Standardization of Precipitation Data**. An extension to all 88 stations is provided in supplemental figure S4.)

timators (MLEs)¹⁶. In this case, the Mahalanobis distance $d_{\Sigma}(\hat{\theta}_a, \hat{\theta}_b) = (\hat{\theta}_b - \hat{\theta}_a)^{\top} \Sigma (\hat{\theta}_b - \hat{\theta}_a)$ obeys a $\chi^2(\text{df} = |\theta| = 3)$ distribution when both parameter estimates are independent draws from the same sampling distribution. Likewise, we can also compare marginal differences to their respective standard deviations, which yields standardized differences, which approximately follow standard normal distributions. In this manner, large standardized differences can indicate differences in an underlying sample distribution, given independent samples.

However, considering that in this case we are *not* dealing in independent samples, but rather different views of the very same sample of precipitation, there is no strict analogy. The standard deviations of the marginal sampling distributions (standard errors) are however a natural “yardstick” to measure differences. Formally, the differences between estimates on the same sample

¹⁶There are ways to create sampling distributions and to calculate confidence intervals [e.g. Kysely (2008) for GEV distributions in particular], but the underlying interpretation is particular to a frequentist outlook rather than a particular implementation.

T-Obs Change	Season	% s.t. SE > 1			% s.t. $ d > 3$
		μ	σ	ξ	
From 17 to 7	SON	10	11	23	13
	DJF	10	16	28	23
	MAM	10	17	27	21
	JJA	7	9	18	9
From 7 to 24	SON	6	8	26	15
	DJF	9	15	28	21
	MAM	8	13	21	14
	JJA	6	12	20	13

TABLE 3. Analogous to Table 1, the columns for location μ , scale σ , and shape ξ are the respective percentage of raingauges for which the standardized difference from the original T-Obs to the new T-Obs is greater than 1. The last column is the percentage of raingauges for which the Mahalanobis distance is greater than 3, where the reference covariance matrix comes from the base T-Obs.

viewed at different T-Obs could be taken to be paired samples, but we cannot specify the theoretical distribution of these differences without a full model of RX . This informality is what makes this an exploration rather than an experiment, but there is much intuition to be drawn from its result about GEV inferences on accumulated quantities.

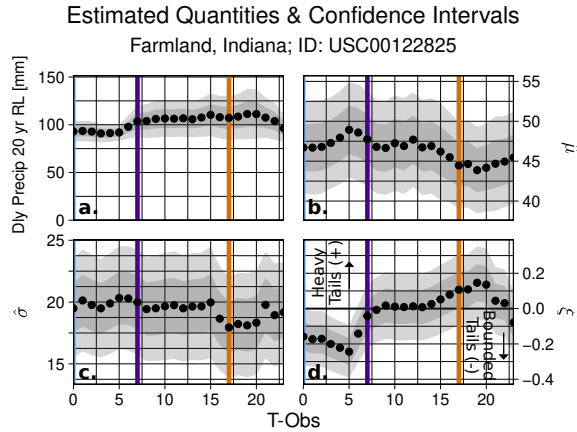


FIG. 7. GEV inferences for daily data at Farmland, Indiana at 24 possible T-Obs; a) 20y daily return level, b) GEV location parameter, c) scale parameter, d) shape parameter; Marginal CIs and 1-SE-wide intervals are underneath each point estimate. Vertical lines denote three T-Obs: orange (5pm), blue (midnight), purple (7am).

Discretization of JJA Maxima at Two T-Obs
Farmland, Indiana; ID: USC00122825

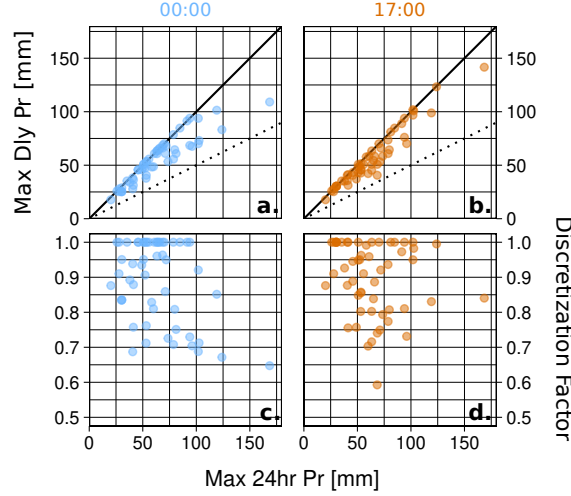


FIG. 8. Example of 24hr and daily precipitation maxima at Farmland, Indiana in JJA; Data from 55 summers are included. a, b: 24hr maxima vs daily maxima recorded at 00:00 and 17:00 respectively. c, d: 24hr maxima vs discretization factor at the same times.

Result: At Farmland, Indiana, the shape parameter estimate $\hat{\xi}$ is quite distinct at the three T-Obs [Fig. 7d]. Consider the 17:00 estimate and its 1-SE and 2-SE intervals. $\hat{\xi}_{24:00}$ and $\hat{\xi}_{07:00}$ are both outside the 1-SE interval. These are the sorts of differences we consider for all parameters and all stations.

In general, it is apparently the shape parameter estimate $\hat{\xi}$ which differs most between the T-Obs [Table 3]. Note that this is relative to the standard errors calculated under the assumption that the BMS arises from a GEV distribution. This clarifies the statistical mechanism of the T-Obs effect. The discretization factor's effect most manifests in the shape parameter which, in particular, affects the tails of the distribution.

d. Experiment 2: Are the Discretization Factor & Precipitation Independent?

Setup: It is clear that T-Obs has a strong *apparent* affect on estimates [Figs 4,7] and their uncertainty [Tables 1,3]. Since parameter estimates, in particular that of the shape $\hat{\xi}$, are sensitive to T-Obs, it is relevant to ask if the 24hr annual maxima X are independent of the proportion we end up measuring R . At Farmland, a comparison of the 24hr maxima x_i to the daily maxima y_i

and discretization factors r_i at midnight and 17:00 both indicate that the proportion we end up measuring depends on the size of the quantity we are trying to measure [Fig 8]. At midnight, the largest 24hr annual maxima are severely under-counted in the daily timeseries, which intuitively explains the estimate of a negative shape parameter (bounded tail) at that time of day. A closer look also shows that 24hr annual maxima are much more likely to be perfectly observed $r = 1$ when 24hr annual maxima x are small at midnight than at 17:00. In this case, after 55 summers, it is sensible to believe that x and r are related, at least if the observations are taken at midnight.

The dichotomy of dependence vs. independence is a sensible concept in this setting, but any test of this must be approached delicately. We do not endorse a particular distribution for R , but it is clear that it has an atom (positive probability) at 1 and a continuous density function covering $(1/2, 1)$. R has a mixed distribution. There is a well-considered test of the null hypothesis that $R \perp\!\!\!\perp X$, which we apply to the three T-Obs and all four seasons [Genest et al. (2019); Nasri et al. (2024)]. If we consider apparent diurnal cycles (especially in JJA) at each location, we would however *not expect* this to manifest uniformly over space, seasons, or T-Obs. Rather, (in)dependence of the 24hr annual maxima and the proportion of each of them that we observe would be mediated by the diurnal cycle. That is, dependence may be conditional.

Result: It turns out that the station-wise (marginal) tests reject the null at $\alpha = 0.05$ rather

Season	No. Station	% Rej.		
		00:00	07:00	17:00
SON	300	07 (20)	06 (15)	03 (14)
DJF	186	03 (11)	02 (19)	02 (15)
MAM	297	04 (16)	03 (17)	03 (15)
JJA	314	11 (22)	01 (16)	03 (17)

TABLE 4. Overall rejection rates of hypothesis tests of independence Genest et al. (2019) of R and X at three T-Obs, both FDR-controlled, and marginal (in parentheses); $\alpha = 1/20$, $\alpha_{\text{FDR}} = 1/10$, and all settings default in R function `MixedIndTests::TestIndCopula()` [Nasri et al. (2024)]

consistently across seasons and T-Obs [Table e]. An established method for controlling for the false discovery rate ($\alpha_{\text{FDR}=0.1}$) discounts many of these rejections, but not all [Benjamini and Hochberg (1995); Wilks (2016)]¹⁷. In this context, it would be unwise to discount dependence of R and X in general.

¹⁷In general, the process for calculating α_{FDR} can be quite noisy. Quite interestingly, the very convincing dependence in figure 8c is considered only marginally significant.

e. Experiment 3: Dependence of Dependence on Diurnality

Setup: If diurnality is to be the explanation of the dependence of R and X , one would need to explain why table does not seem to have very much seasonal or diurnal rhyme or reason. It is so that the strongest evidence for dependence arises in JJA, but on the other hand, the marginal rejection rate is rather constant across seasons and T-Obs (high teens, plus noise). A straightforward way to disentangle this is to scramble the start times of observed events at each station, then repeat the test for independence. At each station for each historical season, positive runs of 24hr total precipitation were assigned random starting hours. Each run was kept intact. The same test for dependence was likewise applied to the randomized series. This is analogous to the general test for diurnality employed in figure 3.

Result: The marginal rejection rates for independence for SON through JJA are 20%, 17%, 17%, and 19%, respectively. It is quite telling that the marginal rejection rates are similar to those we see in the original data across the various T-Obs. A first impression may be that the type I error rate of this test is inflated for the sample sizes we are dealing with, but this is manifestly not the case [**Supplemental Section Type I Error Check for the Test of Independence**]. Rather, the apparent dependence of R and X can arise regardless of a diurnal cycle, which is unfortunate for anybody looking for a tidy, physical explanation. Further study of this dependence is warranted, but the explanation will probably be one of the general nature of discretization of rolling sums of episodically building accumulations rather than one of diurnality.

3. Discussion

a. Synthesis of Results

Inferred large return levels of daily precipitation, given a *single* actual realization (sample) of precipitation, apparently differ substantially from each other, depending on the time of day when raingauges are checked (Exploration 1, Experiment 2). The “statistical mechanism” for this seems to be a noisy aggregation process which unduly influences estimates of the shape parameter $\hat{\xi}$, upon which rare return levels (high quantiles of the response distribution) strongly depend (Exploration 2). We did not find evidence for a diurnal connection to the noisy sampling process (Experiment 3), which consequently does not support the notion that existing inferences are biased nor does it imply anything about an inhomogeneity affecting trends in these rare return levels

(Experiment 1). However, the variation in the shape parameter estimates with the T-Obs, which is markedly larger than that in the location or scale, suggests that estimates of the shape parameter in particular are quite arbitrary (Exploration 2)¹⁸ and not as related to the climate itself as are the other parameters. It seems that the shape parameter acts as a sort of nuisance parameter, taking on whatever value it needs in order to maximize a likelihood function which does not suitably describe the actual data generation process. Overall, this calls into question those purported quantifications of uncertainty of high return levels of daily precipitation which are based upon the GEV family. It is troubling that the very same sample, aggregated slightly differently, routinely results in estimates which are nearly as distinct from each other as estimates which would arise from completely independent samples of the same distribution. This is indicative of a particular kind of model misspecification when asymptotic extreme value distributions (GEV/GP) are applied maxima taken over insufficiently large blocks. However, at this moment, we should take this latter part to be an informed supposition, which is supported by the reasoning in the introduction and buttressed by the results presented here. More practically, we realize that the once-daily sampling of precipitation makes any one observation less meaningful than, for example, a once-daily minimum temperature measurement which is taken at a T-Obs well-coordinated with the diurnal cycle. It may be that daily precipitation values themselves should generally not be considered on their own.

401 *b. Limitations, Generality*

402 Strictly speaking, our results apply to estimates of large return levels of daily precipitation ac-
403 cumulations based on block maximum input data with small block sizes, common in practical
404 data analysis¹⁹. Furthermore, we have only considered the GEV family under two model designs:
405 purely stationary and with trends in scale and location.²⁰ This modelling framework is far from
406 unassailable, and we do not endorse it as the best model for the purpose of estimating large return
407 levels of daily precipitation in general. This being said, its use here as a demonstration is defen-
408 sible insofar as it is customary and tractable [Perica et al. (2011); Coles (2001), and every book
409 of standards which cites NOAA’s Precipitation Frequency Atlas]. Theoretically, the distribution
410 of 24 annual maxima X is probably not GEV, given that the blocks (seasons or years) provide

¹⁸Of course, all parameters are inter-related.

¹⁹Yes, even the results, which do not explicitly invoke GEV are affected, as the focus on annual maxima is rooted in this distributional family.

²⁰A trend in location only as in Risser et al. (2019a) was also considered, but the results were very similar.

411 samples too small for the extremal types theorem to apply [Veneziano et al. (2009)]. However,
 412 even in a hypothetical best case scenario in which we know of a continuous family f which (i)
 413 which approximates the relevant quantiles of X , (ii) has an estimator $\hat{\theta}$ with good small-sample
 414 properties, and (iii) fits well within a framework that allows for nonstationarity in the parameters,
 415 the fact remains that X is not RX , and therefore the discretization factor R ought to be accounted
 416 for. In other words, the model misspecification we have revealed is of practical importance.

417 *c. Specific Commentary*

418 **Trends and Attribution:** It seems that GEV-based assessments of the significance of trends are
 419 quite resistant to the T-Obs inhomogeneity. We specifically checked this for trends in location and
 420 scale because large quantiles of a GEV distribution (and other distributions) are quite insensitive
 421 to a change in location alone [Withers and Nadarajah (2013)]. Such pure location trends were ex-
 422 plored in Risser et al. (2019a). This being said, it does not seem a given that realized magnitudes
 423 of trends are physically interpretable quantities. If we are considering trends relative to a pure
 424 Clausius-Clapeyron 7% per °C baseline, it seems that noise from T-Obs alone would be enough
 425 to foil interpretation. In the event that a trend is detected in 20 year return levels, for instance,
 426 who is to say if its value is 7%, 3%, or 20% [Fig. 6]? Note that confidence intervals of such
 427 estimates, though already wide, are probably understated in the presence of such a model mis-
 428 specification. Interpretation of the magnitude of trends would be safer given observations taken
 429 at a higher sampling rate than once-daily, but on the other hand, daily data provide the longest
 430 and most spatially complete records. The balance of the quality (in this case, adequate sampling
 431 rate) versus quantity (record length and spatial coverage) must be further explored. Collation and
 432 digitization of hitherto undigitized high resolution data should help expand spatial coverage into
 433 the past at select sites. An issue we noticed with the GHCN-hourly dataset is that many airports
 434 are missing or apparently poor quality data from the mid 1960s through late 1970s, which severely
 435 limited our ability to assess trends²¹. Since the data are missing for the same period, and is often
 436 present before and after, the data in the missing period probably exist, but did not make it into the
 437 NOAA collection yet. In addition, there are extensive paper records and metadata from at least
 438 one first-order site (San Diego Airport) which, to our knowledge, have never been digitized, and

²¹There also seems to be an issue soon after the introduction of ASOS platforms, but it may well be that manual and ASOS sensors coexisted for a time at nearby but distinct sites. In this case, a manual raingauge and an ASOS recording gauge may have large disagreements on account of siting characteristics. Overall, a lot of metadata are missing, even at first order sites, so it is difficult to know.

the documentary evidence, including communications with the the Weather Bureau imply that this must be so at other sites as well [WB (1996)].

Spatial Interpolation: The probabilistic gridded product of Risser et al. (2019b) is created through the estimation of parameters of a GEV distribution separately at raingauges, followed by spatial interpolation onto a grid through a second order non-stationary Gaussian process. In this framework, spatially-varying, anisotropic (direction-dependent) relationships of the parameters are allowed. These relationships needed to be inferred under practical constraints, which necessitates an assumed structure of dependence of signal and noise or errors. In that case, the $\hat{\xi}$ was considered to vary isotropically over very long distances, probably because the point estimates appear very noisy and are quite lacking in structure compared to the location and scale parameter estimates. Fully consistent with this, we have realized that the shape parameter estimated at any single station is not representative of the climate of the period when the observations were taken. It may not be so that under the model misspecification, the errors in $\hat{\xi}$ mean out over space to reveal a true underlying signal. Short of a complete specification of R and its relationship to X , a follow up study exploring the spatial variation of $\hat{\xi}$ on BMS data at non-fixed T-Obs should be informative. Of course, there are fewer high temporal resolution stations than there are daily stations, but it may be that a more coherent spatial signal exists when we allow the T-Obs to move to capture the true 24hr maximum at each point.

Connection to Sample Adjustment Factors: The concept of a Sample Adjustment Factor (SAF) is related to the “Discretization Factor” [Weiss (1964); Young and McEnroe (2003); Yoo et al. (2015); Perica et al. (2011)]]]. In particular, for a given aggregation resolution (e.g. 24hrs), a SAF supposedly accounts for the subsampling problem by being multiplied by the precipitation observed at fixed times. In this case, $\text{SAF} = s_o = \mathbb{E}(R^{-1}) \cong 1.15$ and the observations we input into our extreme value analysis are $ys_0 = x$. Notably, s_o is a pre-evaluated constant. It merely rescales all observations by the same proportion, and even a well-chosen constant does little to solve the essential model misspecification issue.

Higher Moments & Random Variable Character: Acknowledging that $r = s^{-1}$ is but a realization of a random variable R is important because it affects the estimate of the shape²² of our observed distribution rather than just that of the location or scale. Oftentimes $r = 1$, so there is an atom of the CDF of R at 1, but it can be as small as $1/2$. Papalexiou et al. (2016) emphasized

²²In general, all moments.

the point that R ought to be thought of as a random variable and that the product RX behaves differently from X^{23} and proposed two distinct ways of considering this.

One essentially continues on the SAF path, but in this case the second moment is also bias-corrected. In particular, they found empirical relationships between the mean and variance of sliding and fixed maxima which were assumed to be invariant in space and T-Obs, depending only on sampling/aggregation resolution. These are used to modify native input data sampled at fixed intervals before GEV parameter estimation. Essentially, the first two moments are bias corrected instead of just the first, as would be the case with a conventional SAF. Under this scheme, the only way in which the RV character of R is relevant is that the coefficient of variation (CV) of the modified data is not equal to that of the native input data. The corrections applied, however, are notably deterministic.

A distinct approach of Papalexiou et al. (2016) acknowledges the RV character of R but immediately gives up on the notion that $\text{Cov}(R, X) \neq 0$. They propose a distribution for R , the bounded exponential distribution with an atom at $r = 1$, which is said to fit observed samples r quite well. Its parameters, like the correction factors they propose, depend upon the resolution of the input data alone. There is no exploration of the relationship of R and X , which undercuts their point that $\text{Cov}(R, X) \neq 0$. Using this distribution, they set up an instructive case study of an annual maximum series of daily precipitation observed at Shasta Dam: random values $\{r_1, r_2, \dots, r_n\}$ were generated from their proposed distribution and multiplied²⁴ by their observed sample $\{y_1, y_2, \dots, y_n\}$. They did this repeatedly and re-estimated GEV parameters for each replicate. The intuition drawn from it is similar to our own study: the very same input data (the very same meteorological history over many decades) can result a wide range of GEV parameter estimates as a result of insufficient sampling of the timeseries. Their figure 11 shows, as does our figure 7 and table 3, that shape parameter estimates $\hat{\xi}$ under different views of the same dataset can cover the entire range of reasonable values of ξ (approximately, -0.1 to 0.3). However, their simulation was conducted with independent R and X . Dependence is not a requirement for R to cause issues, but this leads to an understatement of the problem. It would be useful to expand upon the Papalexiou et al. (2016) model, and put it on a stronger statistical footing²⁵, but we disagree with the notion of geographical universality of the parameters of the distribution of R . Coherent spatial variation it is mean was

²³Namely $\mathbb{E}(RX) \neq \mathbb{E}(R)\mathbb{E}(X)$, which is equivalent to saying that $\text{Cov}(R, X) \neq 0$.

²⁴Our formulation is in reciprocal of their own.

²⁵This is in agreement with Pöschmann et al. (2023)

shown over China as far back as 1997 [van Montfort (1997)] and its seasonal and spatial characteristics are not to be ignored [Appendix A of Dwyer and Reed (1995), Muñoz Proboste (2018)²⁶, Llabrés-Brustenga et al. (2020)].

Shape (or Extremal Index or Heavy Tailedness) and Discretization Under GEV: There is a theoretical argument to be made that discretization does not affect the shape parameter ξ of a GEV distribution. First, we must accept the hypothesis that the block sizes in question (single seasons or years) are large enough for EV theory to apply. If we accept this, then there are conditions under which $\xi_{24\text{hr}}$ and ξ_{dly} would theoretically be equal [Robinson and Tawn (2000)]. Van de Vyver (2015) took a principled stance on this basis and proposed a comprehensive method to solve the discretization problem in this setting. This may well provide a stronger starting point than extension of Papalexiou et al. (2016), so their relative merits should be compared for anybody who wishes to assume that R and X are independent. However, the issue with both of these directions is that they do not address the notion that the GEV shape parameter does seem to be affected by discretization. There are at least two theoretical reasons this could be. One is that the limited block sizes themselves make GEV a poor model for Y or X in the first place [e.g. Veneziano et al. (2009)]. Another is that if R and X are dependent, then X and RX may well have different shapes. In terms of Robinson and Tawn (2000), this would mean that a necessary condition for unvarying shapes under discretization has not been met. Stepping outside of GEV (regularly varying & subexponential distributions) altogether, this would mean that multiplication by R is a random operation which acts on X to modify its obesity [Cooke et al. (2014)].

d. Onwards

Communication of Uncertainty and its Use in Practice: What are reasonable expectations of a model? At the very least, (i) it should provide estimates (return levels) which are physically reasonable. Furthermore, (ii) the output being a transparent function of the input is a requirement for anything except for strictly exploratory data analysis. Beyond this, (iii) measures of uncertainty under the assumption that its underlying premises are true are often demanded. Statistical models with parameters estimated by maximizing likelihood functions promise and provide this, but guarantee nothing more.

²⁶Cited with the background knowledge that predominant storm type is related to geography and season.

526 However, in vernacular culture and practice, it seems that the models are misunderstood and
527 fetishized: they are assigned properties which they do not actually have. Notably, (iv) that a
528 model can provide a general measure of uncertainty for the quantities it is used to estimate. A
529 *mathematical model is in no way “aware” that its underlying premises have been violated.* Even
530 if it were, what use do confidence intervals have to end-users who may well misinterpret them?
531 For example, in the California Department of Water Resources’ manual on urban levee design [CA
532 DWR (2012)], there is the following (annotated) definition:

533 **Definition 3.1** (Assurance). *a measure of confidence that the estimated 200-year water sur-*
534 *face elevation used as the basis for design is equal to or higher than the true 200-year wa-*
535 *ter surface elevation (true by definition, and is an assertion of a frequentist*
536 *interpretation of objective probability). This accounts for uncertainty about the true*
537 *value that arises from fitting frequency curves with small samples of streamflow data (true), us-*
538 *ing imperfect knowledge and imperfect models of the hydrologic and hydraulic system (false).*

539 The first and second parts are inherent to the definition of confidence intervals²⁷. However, it
540 is not clear what any of this would mean to somebody who has never internalized these notions,
541 nor engaged with the long-running debates about their proper role and interpretation [e.g. Birn-
542 baum (1962), Mayo (1981), Ganderberger (2015)] or written a computer program implementing
543 them. Even if this is well understood and accepted to be meaningful, is a confidence interval
544 truly something which provides “assurance” to a design of a levee? Per the manual, this level is
545 apparently used to set the height of levees, and the notion that some assurance against overtop-
546 ping (over what time period?) is provided by the method. Furthermore, (iv) is invoked, meaning
547 numbers calculated by the confidence procedure are assigned properties they do not have. Similar
548 canards and misinterpretations can be found in the California Highway Design Manual section on
549 Hydrology [CalTrans (2020)]²⁸. Further review and textual criticism of engineering manuals is
550 necessary, but so is further study (polling) of how these concepts are understood by engineers in
551 practice (outside of academia). Information provided by the NOAA Precipitation Frequency Atlas
552 [Perica et al. (2011)] should be as fool-proof as possible, and confidence intervals certainly are
553 not. If the goal of these manuals is to produce a standardized recipe to functionally output large

²⁷See Neyman (1937) for the frequentist conception.

²⁸e.g. “Statistical methods, in general, do not require as much subjective judgment to apply as the previously described deterministic methods.” or “The accuracy of statistical methods can also be measured quantitatively.”

(but not overly large) numbers which are somehow tethered to in-situ data, then there are other more straightforward and less theory-laden ways of doing so. It is worth asking how applying a misspecified statistical model or enlisting a confidence interval to a task it was never intended for serves this purpose.

Practical Estimation of High Quantiles: Van de Vyver (2015) seems to provide the best extant solution to the discretization problem, however he assumes that the shape of the distribution is unaffected by discretization. This is not generally true, and it is therefore not a complete solution.

Gaining Intuition on Discretization Noise and High Quantile Estimates: Even if R and X are nonindependent in general, there is still intuition to be gained from the theoretical and empirical properties of $\hat{\theta}_{\text{MLE}}(RX)$ under the assumption that $RX \sim \text{GEV}$. Given the density of the product RX , one could verify that the typical asymptotic properties of MLEs hold true under model misspecification [White (1982)]. The form of the density of $Y = RX$ given independent R and X seems to already have a solution, though grisly manipulations are required. Fox H-function expressions of densities, Mellin transforms, and their inverses should give the density $f(y)$ [Springer (1979)]. Rathie et al. (2023) provides very useful headway in this direction. Even short of the theoretical density of RX being known, empirical studies on generated samples are possible, given a CDF or a stochastic representation.

Role of Daily Observations in Climatology: We conclude that daily precipitation observations, which are awkwardly discretized, have a limited physical meaning compared to both finer and coarser resolution data. Data being discretized (subsampled) at the same or similar timescale to the period over which they are aggregated are confounded by discretization. Studying sequences of hourly precipitation²⁹ with an appropriate stochastic model [e.g. Papalexiou (2018); Weyant et al. (2025)] could give insight into how physical phenomena reflect in longterm statistics. On the coarse resolution side, long-term monthly data, corroborated by daily observations, are best suited to understanding spatial patterns and change over time. Daily observations occupy a liminal space: they are abundant and nominally at a resolution which is useful for natural hazards applications, but are also corrupted from the moment they are recorded by an irreversible, nonlinear discretization process.

Form of an Ideal Solution to the Discretization Problem: A complete solution to the problem should be internally consistent while respecting the following:

²⁹The finest resolution with any semblance of adequate temporal and spatial coverage

584 1. Maximum precipitation observed on a fixed schedule is a random multiple what could have
585 been observed given continuous data

586 2. The proportion observed depends on storm type, and therefore is related to the diurnal and
587 seasonal cycle in general, with independence arising only as a special case

588 Such a solution is needed if the daily records are to be used directly to understand 24 hour accumu-
589 lations. Otherwise, a combination of high-resolution records for subdaily timescales and sensible
590 aggregations of daily observations for daily to superdaily timescales are both well justified for
591 now. We must keep in mind that the spatial density and record length of the once-daily observa-
592 tions far outstrips those of the higher resolution observations, even if all of the latter were to be
593 digitized. It would be foolish to misuse the daily data or let them go to waste. Rather, we must
594 reinterpret them light of their known limitations.

595 *Acknowledgments.*

596 *Data availability statement.* All precipitation data [Menne et al. (2023, 2012b, 2018)] and asso-
597 ciated metadata [McNeill (2011); Vose et al. (2011)] used in this work are freely available from
598 the the National Oceanic and Atmospheric Administration. Data processing (R and shell) scripts
599 specific to this work are archived on GitHub ([https://github.com/aweyant/tobs_daily_](https://github.com/aweyant/tobs_daily_precipitation_stats_issue_paper_data_processing_scripts)
600 [precipitation_stats_issue_paper_data_processing_scripts](https://github.com/aweyant/tobs_daily_precipitation_stats_issue_paper_data_processing_scripts)) and are described in the
601 **Data** appendix. They sometimes depend on more general file reading/writing scripts ([https:](https://github.com/aweyant/weatherAndClimateUtils/tree/main)
602 [//github.com/aweyant/weatherAndClimateUtils/tree/main](https://github.com/aweyant/weatherAndClimateUtils/tree/main)) as well as wrappers/macros
603 for standard GNU programs. The latter are one-liners whose function is apparent from their name.

APPENDIX A

Data

a. Global Historical Climatological Network

The Global Historical Climatology Network (**GHCN**) is a vast collection of surface station observations collated by NCEI from many disparate sources. In the United States, the majority of these records are collected by volunteer observers as part of the Cooperative Observer Program (**COOP**). We accessed the monthly [Menne et al. (2018)], daily [Menne et al. (2012b,a)], and hourly [Menne et al. (2023)] editions in July 2025. The Master Station History Record (**MSHR**) and Publication History Report (**PHR**) are metadatasets from which we can learn about station network membership, relocations, the stated T-Obs, as well as instrumentation & siting conditions [Vose et al. (2011); McNeill (2011)].

b. Standardization of Precipitation Data

1) STATION SET REQUIREMENTS

We composed sets of stations from GHCN fit to our various purposes. The degree of quality control required varies by analysis, so we apply our sieves systematically and flexibly so that each analysis has as large a subset of stations as possible while still being valid. The various steps of analysis and their concomitant requirements are:

- **Extreme Value Analysis (complete samples within each block):** although this is particularly import for the analysis of annual maximum series, the number of values over which a maximum is taken must be comparable between seasons and years. For example, if weather observations are only reported for half of the days in a winter at a southern CA raingauge, then the maximum value for this winter is not comparable to another which had observations every day.
- **Trend Analysis (temporal uniformity):** observations throughout the portion of the record considered must be recorded at a tolerably constant density in time and be homogenous. Multiyear blocks of missing data or changes in instrumentation, gauge siting, or observing practices should be avoided whenever possible.

- **Spatial Analysis (spatial density):** This is purposefully left vague. For any kind of spatial analysis or qualitative or exploratory analysis, the spatial density of stations must be at an appropriate scale to what we are studying. This requirement is generally opposed to the others.

Our present goal is to demonstrate the severity and nature of the interaction of the diurnal cycle (a natural system) with the varying and changing practices of precipitation observers contributing to the daily precipitation record in CONUS (a human/bureaucratic system). This informs our application of the sieves.

For our “snapshot” EVA, we require that blocks be complete, but not that values be uniform over time. If we wish to compare EVA inferences (AMS-GEV or POT-GP) of P_{24} at different times of day, it does not matter very much which exact years are represented in our set, as long as they represent the issue at hand well enough. In this case, the assumption is that the years/blocks which have complete hourly observations are representative of the years for which we lack such data.

For the trend EVA, we further wished to require temporal uniformity, insofar as sampling density is concerned. However, the GHNC-hourly dataset systematically has missing data from 1965 through the late 1970s at many airports. This forced us to drop this requirement in this case. Inhomogeneities other than those caused by the time of observation are ignored. For now, we are assuming that siting and instrumentation inhomogeneities, being present at all hours of the day, would not affect the results of what is fundamentally a paired experiment at each site. While it is conceivable that a siting or instrumentation inhomogeneity particularly affects observations at certain times of day, we are not presently considering this.

With the principles and limitations thus outlined, proceed with the precise implementation of the sieves and the resultant subsets. This proceeds hierarchically with the scale of aggregation, from months down to hours.

2) GHCN-MONTHLY

We offload two spatial aspects of our station filtering to the National Center for Environmental Information (NCEI). Within the GHCN-m dataset, we consider two quality control flags. “S” indicates that “the number of nonzero precipitation days is grossly inconsistent with the number

660 at neighbouring stations” and “T” indicates that “the (monthly precipitation value) at this location
661 is either much smaller or much large than neighbouring values.”

662 3) GHCN-DAILY

663 Daily precipitation values are eliminated (set to NA/missing) whenever their GHNC-d measure-
664 ment flag is “A” (precipitation is formed from a multi-day total) or if any GHCN-d data quality
665 flags are present. With an eye toward overall precipitation frequency and extreme value analysis,
666 we also eliminate any observations in a month for which the GHCN-m flag is “S” or “T”.
667 The T-Obs, which is supposed to be presented alongside each observation, is often missing. It is
668 possible that some of these were provided by observers but not digitized. Whenever the T-Obs is
669 present, it is retained and we call it the “GHCN-d T-Obs”.

670 4) EXCLUSION SIEVES

- 671 • **Openness and Record Length:** A station must not be listed as “closed” or “abandoned” in
672 its publication history report (PHR), and must have a daily precipitation record spanning at
673 least 60 years. This ensures that the stations in our set are all still recording observations and
674 have long records, so that they can be used to provide historical context to events which have
675 occurred as recently as in the past month.
- 676 • **Strict Seasonal Completeness (complete samples within each block):** Every season in-
677 cluded in the EVA or the identification of diurnal cycles must itself be complete. Complete
678 seasons may not have more than 27 days of missing values. Note that entire months not pass-
679 ing NCEI’s spatial consistency checks are not already culled by this point. Therefore, any
680 three-month season which contains one month of missing values (on account of the GCHN-
681 m flags “S” or “T”) will be eliminated. However, up to 27 “missing” values are allowed
682 because flags “S” or “T” together account for any large nonzero precipitation observations
683 being missed in a given month. IN regions with marked dry seasons, it is not a major issue
684 to retain a station with missing values (true zeroes), so long as it has passed the monthly QC
685 checks. To be even more sure that the seasonal daily maximum value was indeed recorded, the
686 difference between the seasonal total formed from the daily values and the “native” GHCN-m
687 seasonal total is compared to the seasonal daily maximum. If the daily seasonal maximum

is smaller than this difference, then the only way that a true seasonal daily maximum could have been overlooked is if a missing seasonal maximum was not severe enough to make the seasonal total fail the spatial monthly consistency check “T”.

- **Epochal Integrity (temporal uniformity):** For trend analysis, timeseries integrity is determined within 30-year epochs, as would be used to calculate “30 year normals”. We count back from the present wateryear 2025. E2025 denotes the 30-year epoch (1996,2025]. E1965 is a “rump epoch”, extending only back to 1948, when a substantial portion of GHCN-d records changed from a punchcard format which was easier to digitize [Kunkel et al. (2005)]. A timeseries is considered to have “integrity in all seasons” in an (rump) epoch if, for each three month season, no more than (3) 5 of the seasons in 30 (18) years contain GHCN-m “T” or “S” quality flags. In this manner, the climatology of each season is well represented, but any particular year may have different seasons missing. Ideally, if there are missing seasons, they are uniformly spread over the years, but this is unlikely in practice. Inactive seasons tend to be consecutive, and are sometimes at the beginning or end of a record. The calculation of trends requires integrity all all historical epochs: E2025, E1995, and E1965, while “snapshot” values only require that there be at least 30 complete seasons.

5) GHCN-HOURLY

GHCN-h, despite its name, is partially a sub-hourly dataset. This is especially apparent at airport stations, which can issue many special reports in an hour at irregular intervals. Every month, the most common minute of observations is identified, and all other observations are filtered out, which results in a regularly sampled hourly dataset. In the event that a data logging system changes within a month, this will result in a valid month of data being truncated, but switching of automatic datalogging system happens so seldomly that we ignore this. Hourly totals recorded before minute 30 are credited to the previous hour.

P_{24} are formed as rolling sums of 24 hourly observations. In case there are missing observations, it is ensured that P_{24} is indeed formed from consecutive hours.

A season’s worth of hourly data is considered “reasonably complete” if the seasonal total calculated from P_{24} is similar to the total calculated from the daily data over the same dates. These totals are similar if their relative difference, with the daily data as the base, has an absolute value of less

than 10%. This allows for differences between possibly distinct gauges (e.g. a recording tipping bucket alongside a standard 8" non-recording gauge) or precipitation fell in the very first or last few minutes of a season. Most importantly, the diurnal cycle and heaviest precipitation episode for each season is faithfully represented. For the main results, P_{24} at different times are compared to each other rather than daily data, so biases in the recording (sub-daily) instruments compared to the non-recording (daily) instruments are not particularly concerning.

6) STATION SETS

Ultimately, we obtained the station sets in Table A1.

Set	Size	Use
ghcnd-open-conus-60y-qc-all-season-integrity-30y	4406	-
ghcnd-open-conus-60y-qc-all-season-integrity-all-epoch	1228	-
ghcnh-30y-reasonably-complete-ghcnd-open-conus-60y-qc-30y	395	Stationary EVA Diurnal Cycle
ghcnh-45y-reasonably-complete-ghcnd-open-conus-60y-qc-all-season-integrity-all-epoch	88	Nonstationary EVA

TABLE A1. Station sets used, their size, and their purpose. The names of the stations come indicate the sieves applied to them.

APPENDIX B

Methods

a. Determination of T-Obs from Hourly Data

Ideally, there should be a T-Obs recorded alongside each daily observation. In this case, the observer would be asserting each day that the observation was indeed taken at hour h on day d . This is sometimes the case with the GHCN-daily observations, and this T-Obs is written as Measurement Flag #4. However, the means of reporting observations has changed many times over the years, such that at times a general hour h is attributed to entire months at a time. Sometimes this is listed in the Publication History Report (PHR) even when it is not available alongside the observations themselves. We may consider these daily T-Obs declarations to be more trustworthy than more general (monthly/annual) ones. We will call the daily T-Obs *T-Obs Daily* and the more general T-Obs *T-Obs Meta*. If T-Obs Daily conflicts with T-Obs Meta, we default to T-Obs Daily.

For the stations which also provide hourly data, we determine the h for which the 24hr totals align best with the daily totals. First, since dates of precipitation can be offset by one day in either direction³⁰, we correlate 24hr precip at each T-Obs h to the lag, current, and lead daily value. The hour with the highest correlation is taken to be the probable T-Obs. We call this *T-Obs Hourly*. This method of determining T-Obs reveals that the given T-Obs is sometimes incorrect for years at a time. However, given that recording (hourly) and nonrecording (daily) instruments are different, and that observations are not always taken at the top of the hour, these inferred *T-Obs Hourly* vary by an hour or two whenever observers are indeed perfectly on schedule. We therefore convert each T-Obs to a T-Obs category before tracking T-Obs over time or comparing the three different types of T-Obs to each other. The T-Obs are compared, in decreasing order of preference, as: *T-Obs Hourly*, *T-Obs Daily*, *T-Obs Meta*.

b. Extreme Value Inference

Distribution: The parametric family used for inferences on block maximum series (BMS) data is the classic generalized extreme value (GEV) distribution in the parametrization of Coles (2001).

³⁰Observers have always been instructed, since at least before WB (1915), to always record daily precipitation on the day they recorded it, but the cited manual, as well as more recent editions indicate that this is directive is often disobeyed.

T-Obs Category	Time Range
Morning	(02:00, 10:00]
Midday	(10:00, 14:00]
Evening	(14:00, 22:00)
Midnight	[22:00, 02:00]

TABLE B1. T-Obs Categories used when considering changes in the station network, e.g. Supplemental Figures S1 and S2.

Its CDF and n -block return levels are given by equations (B1) and (B2). The parameters (μ, σ, ξ) are called the “location”, “scale”, and “shape”, respectively.

$$F(x) = \exp \left\{ - \left[1 + \xi \left(\frac{x - \mu}{\sigma} \right) \right]^{-\frac{1}{\xi}} \right\}, \text{ where} \quad (\text{B1})$$

$$x \in \{\mathbb{R} \mid 1 + \xi(x - \mu) > 0\}, \mu \in \mathbb{R}, \xi \in \mathbb{R}, \text{ and } \sigma \in \mathbb{R}_{>0}$$

$$z_n = \begin{cases} \mu - \frac{\sigma}{\xi} \left[1 - \left\{ -\log \left(1 - \frac{1}{n} \right) \right\}^{-\xi} \right] & \xi \neq 0 \\ \mu - \sigma \log \left\{ -\log \left(1 - \frac{1}{n} \right) \right\} & \xi = 0 \end{cases} \quad (\text{B2})$$

Parameter Estimation, Vector Generalized Linear Model (VGLM): Parameters are estimated in R [R Core Team (2024)] by maximizing the GEV likelihood function `gevff()` with the `vglm()` in the package VGAM, version 1.1-13 [Yee (2015)]. This is done through iteratively reweighted least squares (**IRLS**) [Yee and Stephenson (2007); Yee (2015)] in both the stationary and nonstationary cases. The nonstationary case in Experiment 1 is similar to Risser et al. (2019a), but we also simultaneously estimated a slope for the scale parameter, in light of Withers and Nadarajah (2013). Both the location μ and scale σ are linearly related to the year of the block. The default configurations, including the selection of starting values and link functions are left as package defaults, as they are well considered and convergence was successful in general whenever 0-inflated (chosen here to mean 15 or more years of BMS precipitation less than $1/10$ of an inch) BMS were eliminated.

References

- Benjamini, Y., and Y. Hochberg, 1995: Controlling the false discovery rate: A practical and powerful approach to multiple testing. *Journal of the Royal Statistical Society: Series B (Methodological)*, **57** (1), 289–300, <https://doi.org/https://doi.org/10.1111/j.2517-6161.1995.tb02031.x>, <https://rss.onlinelibrary.wiley.com/doi/pdf/10.1111/j.2517-6161.1995.tb02031.x>.
- Bickel, P., and K. Doksum, 2015: *Mathematical Statistics: Basic Ideas and Selected Topics*, Vol. 1. 2nd ed., Chapman and Hall, <https://doi.org/\url{https://doi.org/10.1201/b18312}>.
- Birnbaum, A., 1962: On the foundations of statistical inference. *Journal of the American Statistical Association*, **57** (298).
- CA DWR, 2012: *Urban Levee Design Criteria*. URL https://cawaterlibrary.net/wp-content/uploads/2017/05/ULDC_May2012.pdf, accessed 3 Sep 2025.
- CalTrans, 2020: *California Highway Design Manual: Ch 810 - Hydrology*. California Dept. of Transportation, 7th ed., accessed 18 August 2025.
- Coles, S., 2001: *An Introduction to Statistical Modeling of Extreme Values*. 1st ed., Springer London, <https://doi.org/https://doi.org/10.1007/978-1-4471-3675-0>.
- Cooke, R. M., D. Nieboer, and J. Misiewicz, 2014: *Fatness of Tail*. John Wiley and Sons, Ltd, <https://doi.org/https://doi.org/10.1002/9781119054207>.
- Domonkos, P., 2024: Relative homogenization of climatic time series. *Atmosphere*, **15** (8), <https://doi.org/10.3390/atmos15080957>.
- Dwyer, I., and D. Reed, 1995: Report no. 123: Allowance for discretization in hydrological and environmental risk estimation.
- Gandenberger, G., 2015: A new proof of the likelihood principle. *The British Journal for the Philosophy of Science*, **66** (3), 475–503, <https://doi.org/10.1093/bjps/axt039>.
- Genest, C., J. G. Nešlehová, B. Rémillard, and O. A. Murphy, 2019: Testing for independence in arbitrary distributions. *Biometrika*, **106** (1), 47–68, <https://doi.org/10.1093/biomet/asy059>, https://academic.oup.com/biomet/article-pdf/106/1/47/27774584/asy059_supp.pdf.

795 Kunkel, K. E., D. R. Easterling, K. Hubbard, K. Redmond, K. Andsager, M. C. Kruk, and M. L.
796 Spinar, 2005: Quality control of pre-1948 cooperative observer network data. *Journal of Atmo-*
797 *spheric and Oceanic Technology*, **22 (11)**, 1691 – 1705, <https://doi.org/10.1175/JTECH1816.1>.

798 Kysely, J., 2008: A cautionary note on the use of nonparametric bootstrap for estimating uncer-
799 tainties in extreme-value models. *Journal of Applied Meteorology and Climatology*, **47 (12)**,
800 3236 – 3251, <https://doi.org/10.1175/2008JAMC1763.1>.

801 Llabrés-Brustenga, A., A. Rius, R. Rodríguez-Solà, and M. C. Casas-Castillo, 2020: Influence
802 of regional and seasonal rainfall patterns on the ratio between fixed and unrestricted measured
803 intervals of rainfall amounts. *Theoretical and Applied Climatology*, **140**.

804 Mayo, D. G., 1981: In defense of the neyman-pearson theory of confidence intervals. *Philosophy*
805 *of Science*, **48 (2)**, 269–280.

806 McNeill, S., 2011: Publication station history report (phr) for coop elements. National Centers for
807 Environmental Information, NESDIS, NOAA, U.S. Department of Commerce.

808 Menne, M. J., I. Durre, R. S. Vose, B. E. Gleason, and T. G. Houston, 2012a: An overview of
809 the global historical climatology network-daily database. *Journal of Atmospheric and Oceanic*
810 *Technology*, **29 (7)**, 897 – 910, <https://doi.org/10.1175/JTECH-D-11-00103.1>.

811 Menne, M. J., C. N. Williams, B. E. Gleason, J. J. Rennie, and J. H. Lawrimore, 2018: The
812 global historical climatology network monthly temperature dataset, version 4. *Journal of Cli-*
813 *mate*, **31 (24)**, 9835 – 9854, <https://doi.org/10.1175/JCLI-D-18-0094.1>.

814 Menne, M. J., and Coauthors, 2012b: Global historical climatology network - daily (ghcn-daily),
815 version 3. NOAA National Climatic Data Center, accessed 11 July 2025, [https://doi.org/10.](https://doi.org/10.7289/V5D21VHZ)
816 [7289/V5D21VHZ](https://doi.org/10.7289/V5D21VHZ).

817 Menne, M. J., and Coauthors, 2023: Global historical climatology network-hourly (ghcnh), ver-
818 sion 1. Accessed 11 July 2025, <https://doi.org/10.25921/jp3d-3v19>.

819 Muñoz Proboste, P. I., 2018: Effects of storm type on the variability of rainfall sampling ad-
820 justment factors. Master’s thesis, University of Memphis, available at [https://digitalcommons.](https://digitalcommons.memphis.edu/etd/1854/)
821 [memphis.edu/etd/1854/](https://digitalcommons.memphis.edu/etd/1854/).

- 822 Nasri, B. R., B. N. Remillard, J. G. Neslehova, and C. Genest, 2024: *MixedIndTests:*
823 *Tests of Randomness and Tests of Independence*. URL [https://CRAN.R-project.org/package=](https://CRAN.R-project.org/package=MixedIndTests)
824 *MixedIndTests*, r package version 1.2.0.
- 825 Neyman, J., 1937: Outline of a theory of statistical estimation based on the classical theory of
826 probability. *Philosophical Transactions of the Royal Society of London. Series A, Mathematical*
827 *and Physical Sciences*, **236 (767)**, 333–380, <https://doi.org/10.1098/rsta.1937.0005>.
- 828 Papalexiou, S. M., 2018: Unified theory for stochastic modelling of hydroclimatic processes:
829 Preserving marginal distributions, correlation structures, and intermittency. *Advances in Water*
830 *Resources*, **115**, 234–252, [https://doi.org/https://doi.org/10.1016/j.advwatres.2018.02.013](https://doi.org/10.1016/j.advwatres.2018.02.013).
- 831 Papalexiou, S. M., Y. G. Dialynas, and S. Grimaldi, 2016: Hershfield factor revisited: Correcting
832 annual maximum precipitation. *Journal of Hydrology*, **542**, 884–895, [https://doi.org/https://doi.](https://doi.org/10.1016/j.jhydrol.2016.09.058)
833 [org/10.1016/j.jhydrol.2016.09.058](https://doi.org/10.1016/j.jhydrol.2016.09.058).
- 834 Perica, S., and Coauthors, 2011: NOAA atlas 14 volume 6 version 2.0, precipitation-frequency
835 atlas of the United States, California. NOAA, National Weather Service, Silver Spring, MD.
- 836 Pöschmann, J., R. Kronenberg, and C. Bernhofer, 2023: Variability of sampling adjustment factors
837 for extreme rainfall in germany. *Theoretical and Applied Climatology*, **153**, [https://doi.org/https:](https://doi.org/10.1007/s00704-023-04511-3)
838 [//doi.org/10.1007/s00704-023-04511-3](https://doi.org/10.1007/s00704-023-04511-3).
- 839 R Core Team, 2024: *R: A Language and Environment for Statistical Computing*. Vienna, Austria,
840 R Foundation for Statistical Computing, URL <https://www.R-project.org/>.
- 841 Rathie, P. N., L. C. d. S. M. Ozelim, F. Quintino, and T. A. d. Fonseca, 2023: On the extreme value
842 h-function. *Stats*, **6 (3)**, 802–811, <https://doi.org/10.3390/stats6030051>.
- 843 Risser, M. D., C. J. Paciorek, T. A. O’Brien, M. F. Wehner, and W. D. Collins, 2019a: Detected
844 changes in precipitation extremes at their native scales derived from in situ measurements. *Jour-*
845 *nal of Climate*, **32 (23)**, 8087 – 8109, <https://doi.org/10.1175/JCLI-D-19-0077.1>.
- 846 Risser, M. D., C. J. Paciorek, M. F. Wehner, T. A. O’Brien, , and W. D. Collins, 2019b: A proba-
847 bilistic gridded product for daily precipitation extremes over the united states. *Climate Dynam-*
848 *ics*, **53**, 2517 – 2538, [https://doi.org/0.1007/s00382-019-04636-0](https://doi.org/10.1007/s00382-019-04636-0).

- Robinson, M. E., and J. A. Tawn, 2000: Extremal analysis of processes sampled at different frequencies. *Journal of the Royal Statistical Society: Series B (Statistical Methodology)*, **62** (1), 117–135, <https://doi.org/https://doi.org/10.1111/1467-9868.00223>, <https://rss.onlinelibrary.wiley.com/doi/pdf/10.1111/1467-9868.00223>.
- Springer, M. D., 1979: *The Algebra of Random Variables*. Probability and Statistics, Wiley.
- St. Laurent, M., 2020: NOAA atlas 14 precipitation frequency atlas of the United States. Presented at the Northeast Regional Climate Center Workshop.
- Van de Vyver, H., 2015: On the estimation of continuous 24-h precipitation maxima. *Stochastic Environmental Research and Risk Assessment*, **29**, <https://doi.org/https://doi.org/10.1007/s00477-014-0912-5>.
- van Montfort, M. A., 1997: Concomitants of the Hershfield factor. *Journal of Hydrology*, **194** (1), 357–365, [https://doi.org/https://doi.org/10.1016/S0022-1694\(96\)03212-X](https://doi.org/https://doi.org/10.1016/S0022-1694(96)03212-X).
- Veneziano, D., A. Langousis, and C. Lepore, 2009: New asymptotic and preasymptotic results on rainfall maxima from multifractal theory. *Water Resources Research*, **45** (11), <https://doi.org/https://doi.org/10.1029/2009WR008257>, <https://agupubs.onlinelibrary.wiley.com/doi/pdf/10.1029/2009WR008257>.
- Vose, R. S., S. McNeill, K. Thomas, and E. Shepherd, 2011: Enhanced master station history report, version 3. NOAA National Climatic Data Center, accessed May 2023, <https://doi.org/10.7289/V5NV9G8D>.
- WB, 1915: *W.B. No. 539 Instructions for Cooperative Observers: Circulars B and C*. Washington, D.C., U.S. Dept. of Agriculture Instrument Division, 5th ed.
- WB, 1996: Weather bureau records for San Diego. Accessed December 2024 in the special collections of the Love Library, San Diego State University.
- Weiss, L. L., 1964: Ratio of true to fixed-interval maximum rainfall. *Journal of the Hydraulics Division*, **90** (1), 77–82, <https://doi.org/10.1061/JYCEAJ.0001008>.

- 874 Weyant, A., A. Gershunov, A. K. Panorska, T. J. Kozubowski, and J. Kalansky, 2025: A holistic
875 stochastic model for precipitation events. *Scientific Reports*, **15**, [https://doi.org/10.1038/](https://doi.org/10.1038/s41598-024-77031-3)
876 [s41598-024-77031-3](https://doi.org/10.1038/s41598-024-77031-3).
- 877 White, H., 1982: Maximum likelihood estimation of misspecified models. *Econometrica*, **50** (1),
878 1–25.
- 879 Wilks, D. S., 2016: “the stippling shows statistically significant grid points”: How research results
880 are routinely overstated and overinterpreted, and what to do about it. *Bulletin of the American*
881 *Meteorological Society*, **97** (12), 2263 – 2273, <https://doi.org/10.1175/BAMS-D-15-00267.1>.
- 882 Wilson, P. S., and R. Toumi, 2005: A fundamental probability distribution for heavy rainfall.
883 *Geophysical Research Letters*, **32** (14), [https://doi.org/https://doi.org/10.1029/2005GL022465](https://doi.org/10.1029/2005GL022465).
- 884 Withers, C. S., and S. Nadarajah, 2013: Asymptotic behavior of the maximum from distributions
885 subject to trends in location and scale. *Statistics and Probability Letters*, **83** (10), 2143–2151,
886 [https://doi.org/https://doi.org/10.1016/j.spl.2013.06.001](https://doi.org/10.1016/j.spl.2013.06.001).
- 887 Yee, T. W., 2015: *Vector Generalized Linear and Additive Models: With an Implementation in R*.
888 Springer, New York, USA.
- 889 Yee, T. W., and A. G. Stephenson, 2007: Vector generalized linear and additive extreme value
890 models. *Extremes*, [https://doi.org/https://doi.org/10.1007/s10687-007-0032-4](https://doi.org/10.1007/s10687-007-0032-4).
- 891 Yoo, C., C. Jun, and C. Park, 2015: Effect of rainfall temporal distribution on the conversion
892 factor to convert the fixed-interval into true-interval rainfall. *Journal of Hydrologic Engineering*,
893 **20** (10), 04015 018, [https://doi.org/10.1061/\(ASCE\)HE.1943-5584.0001178](https://doi.org/10.1061/(ASCE)HE.1943-5584.0001178).
- 894 Young, C. B., and B. M. McEnroe, 2003: Sampling adjustment factors for rainfall recorded at
895 fixed time intervals. *Journal of Hydrologic Engineering*, **8** (5), 294–296, [https://doi.org/10.1061/](https://doi.org/10.1061/(ASCE)1084-0699(2003)8:5(294))
896 [\(ASCE\)1084-0699\(2003\)8:5\(294\)](https://doi.org/10.1061/(ASCE)1084-0699(2003)8:5(294)).

**Supplementary Material for “Noisy Sampling Inherent to Daily
Precipitation Observations and Implications About Return Level
Inferences”**

Alexander Weyant,^a Anna Panorska,^b Alexander Gershunov,^a Rachel Clemesha,^a

^a *Scripps Institution of Oceanography*

^b *University of Nevada, Reno*

Corresponding author: Alexander Weyant, aweyant@ucsd.edu

8 ABSTRACT:

9 1. T-Obs in the CONUS Raingauge Network

Year	Station Network	Recommended T-Obs	Source
1915	COOP	Sunset	WB (1915)
1962, 1970, 1972	COOP	If one record per day: PRCP only → 6-8a.m. TEMP only → evening TEMP & PRCP → evening preferred, but morning implied to be customary If possible, separate T-Obs for TEMP and PRCP is considered ideal.	WB (1962) NWS (1970) NWS (1972)
1989	COOP	One record per day preferred. PRCP only → 7a.m. TEMP Only → 6p.m. TEMP & PRCP → 6p.m. TEMP and PRCP to be observed simultaneously; local NWS weighs in as to when.	NWS (1989)
2020	CoCoRaHS	7a.m.	Hildberg (2020)
2023	COOP	7a.m. preferred , but 5-8p.m. permissible	NWS (2023)
2025	COOP	Not specified, but differing PRCP & TEMP T-Obs allowed.	NWS (2025)

TABLE S1. An abbreviated history of recommended daily observation times for volunteer observers.

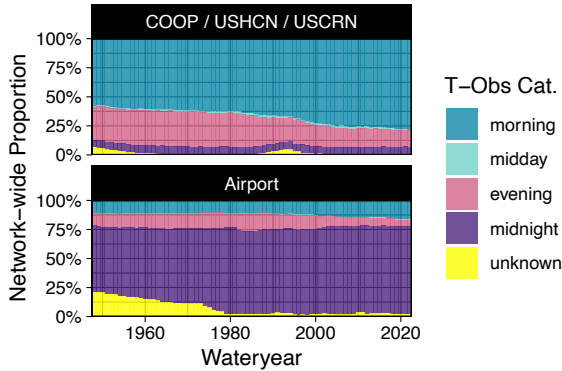


FIG. S1. Network-wide proportions of T-Obs by water year; T-Obs information is favored in increasing preference as: stated in PHR ; given by observer ; determined directly from a comparison of hourly and daily data. See **Data** and **Methods** in the main text. Note that the overall size of the network remained essentially constant throughout this period, so proportions are valid and comparable.

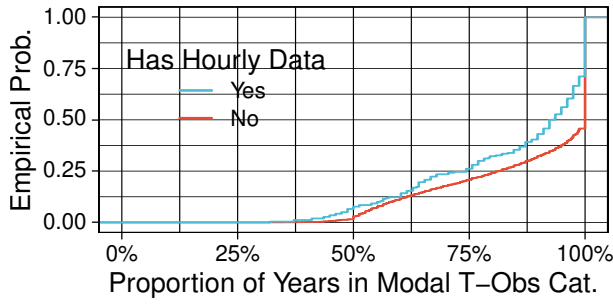


FIG. S2. The network-wide empirical CDFs of the proportion of years in the record for which the T-Obs was in the most common category for each station. A station with 60 years of data, 45 of which have a morning T-Obs, would have a value of $\frac{45}{60}=75\%$. The station network is broken into components which have at least 20 years of complete hourly data (blue) and those which do not (red).

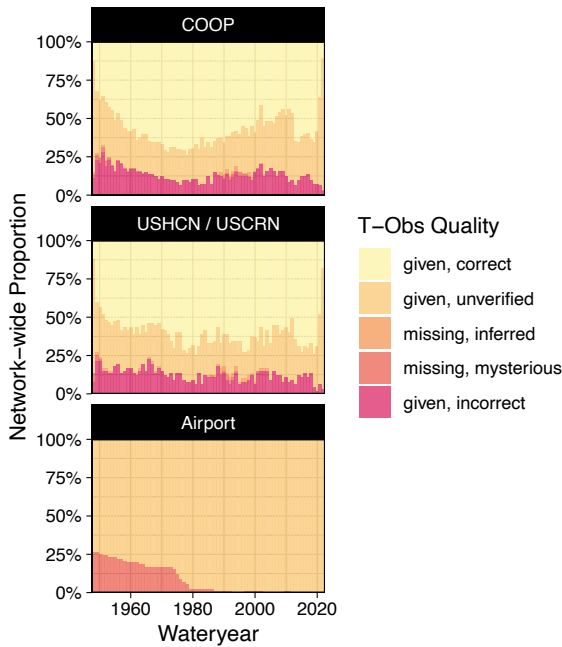


FIG. S3. Quality of given T-Obs data by station network.

18 2. Type I Error Check for the Test of Independence

19 We performed a simulation to make sure that the hypothesis test of R being independent of X
20 [Genest et al. (2019); Nasri et al. (2024)] does not have an inflated Type I error rate in this setting.
21 This is merely a sanity check and to allay any concerns as to this matter. In any case, it is always
22 good to check code that is not your own. However, one would actually reasonably expect an
23 inflated Type II error rate for this type of test, as the alternative hypothesis of dependence is rather
24 vague.

25 In any case, we generated $N = 250$ replicate samples of $n = 30$ random
26 $\text{GEV}(\mu = 0, \sigma = 1, \xi = 1/10)$ and $\text{ABddExp}(p_{\text{atom}} = 1/4, \text{scale} = 1/4)$ (“atomic bounded ex-
27 ponential”). The parameter values for the atomic bounded exponential were chosen to be
28 round and reasonably near those shown of Papalexiou et al. (2016). In this case the mean of
29 R is approximately 1.18. We applied the general purpose test of independence for mixed type
30 distributions to each replicate in the `MixedIndTest` package’s default settings. Ultimately, 6% of
31 the estimated p-values were below 5%, our chosen α , so the test has a well calibrated Type I error
32 rate for our purposes.

Season	No. St.	Dly.	17	Dly., not 17	17:00, not Dly.	17 to 07	17 to 24
SON	88	14	12	4	2	10	13
DJF	88	11	9	5	3	8	11
MAM	88	15	10	5	0	11	9
JJA	82	10	6	6	2	4	3

TABLE S2. Representative results of the paired T-Obs change experiment for location trends. For each season, the total number of stations is reported, followed by the number of stations in each season for which a (marginally) significant ($\alpha = 0.05$) slope of shape parameter was inferred on the daily data and the hourly data aggregated daily at 17:00. The next two columns report disjunctions of these counts, and the last two columns report the number of stations with significant location trends under the conditions that the T-Obs changed halfway through the record.

3. Misc

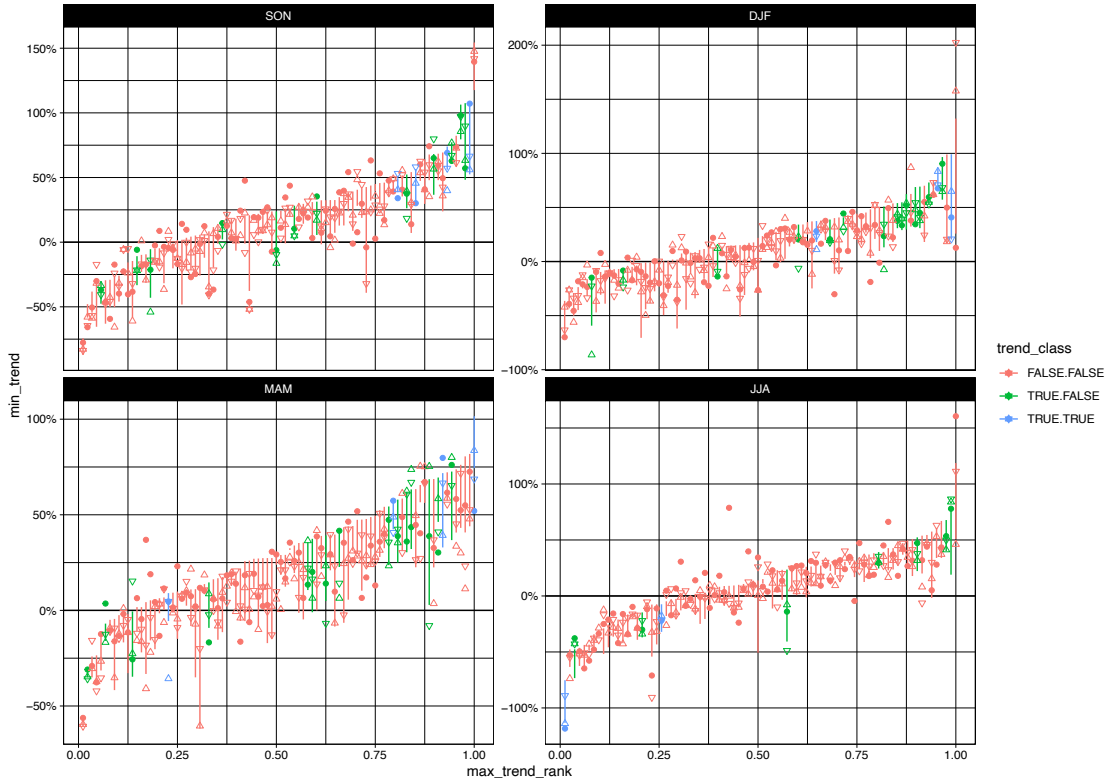


FIG. S4. (An extension of figure 6 to all stations included in the trend T-Obs treatment experiment) Magnitudes of detected trends of 20y return levels, expressed as return level in the final year minus return level in the first year divided by the mean over all years; Each vertical line segment corresponds to a raingauge. The line segments cover denote the min and max magnitude for each station, the solid dots show the corresponding daily value, the up-pointing triangle the switch condition 17:00 → 24:00, and the downward pointing triangle 17:00 → 07:00. Due to missing data in many of the series, the magnitudes of these trends are not to be taken outside of their context.

References

- Genest, C., J. G. Nešlehová, B. Rémillard, and O. A. Murphy, 2019: Testing for independence in arbitrary distributions. *Biometrika*, **106** (1), 47–68, <https://doi.org/10.1093/biomet/asy059>, https://academic.oup.com/biomet/article-pdf/106/1/47/27774584/asy059_supp.pdf.
- Hildberg, S., 2020: The importance of observation time. Accessed: 2025-06-26, <https://cocorahs.blogspot.com/2020/06/the-importance-of-observation-time.html>.

53 Nasri, B. R., B. N. Remillard, J. G. Neslehova, and C. Genest, 2024: *MixedIndTests:*
54 *Tests of Randomness and Tests of Independence*. URL [https://CRAN.R-project.org/package=](https://CRAN.R-project.org/package=MixedIndTests)
55 *MixedIndTests*, r package version 1.2.0.

56 NWS, 1970: *Observing Handbook No. 2, Substation Observations (Supercedes Circular B)*. Silver
57 Spring, Maryland, Dept. of Commerce, 1st ed.

58 NWS, 1972: *Observing Handbook No. 2, Substation Observations (Supercedes Circular B)*. Silver
59 Spring, Maryland, Dept. of Commerce, 2nd ed.

60 NWS, 1989: *Handbook No. 2: Cooperative Station Observations*. Silver Spring, Maryland, Dept.
61 of Commerce, 1st ed., accessed from <https://novalynx.com/manuals/coophandbook2.pdf> on 26
62 Jun 2025.

63 NWS, 2023: *Cooperative Station Observations and Maintenance (NWS Manual 10-1315)*.

64 NWS, 2025: *Cooperative Program Management and Operations (NWS Instruction 10-1307)*.
65 Accessed from https://www.weather.gov/media/directives/010_pdfs/pd01013007curr.pdf on 26
66 June 2025.

67 Papalexiou, S. M., Y. G. Dialynas, and S. Grimaldi, 2016: Hershfield factor revisited: Correcting
68 annual maximum precipitation. *Journal of Hydrology*, **542**, 884–895, [https://doi.org/https://doi.](https://doi.org/10.1016/j.jhydrol.2016.09.058)
69 [org/10.1016/j.jhydrol.2016.09.058](https://doi.org/10.1016/j.jhydrol.2016.09.058).

70 WB, 1915: *W.B. No. 539 Instructions for Cooperative Observers: Circulars B and C*. Washington,
71 D.C., U.S. Dept. of Agriculture Instrument Division, 5th ed.

72 WB, 1962: *Instructions for Climatological Observers, Circular B*. Washington, D.C., Government
73 Printing Office, 11th ed., access from <https://www.analogweather.com> on 26 Jun 2025.